



# MRI of diffuse liver disease: characteristics of acute and chronic diseases

Surya Chundru, Bobby Kalb, Hina Arif-Tiwari, Puneet Sharma, James Costello, Diego R. Martin

## ABSTRACT

Diffuse liver disease, including chronic liver disease, affects tens of millions of people worldwide, and there is a growing need for diagnostic evaluation as treatments become more readily available, particularly for viral liver diseases. Magnetic resonance imaging (MRI) provides unique capabilities for noninvasive characterization of the liver tissue that rival or surpass the diagnostic utility of liver biopsies. There has been incremental improvement in the use of standardized MRI sequences, acquired before and after administration of a contrast agent, for the evaluation of diffuse liver disease and the study of the liver parenchyma and blood supply. More recent developments have led to methods for quantifying important liver metabolites, including lipids and iron, and liver fibrosis, the hallmark of chronic liver disease. Here, we review the MRI techniques and diagnostic features associated with acute and chronic liver disease.

**M**agnetic resonance imaging (MRI) provides superior characterization of disease processes and masses in the liver compared with computed tomography (CT) (1) but requires attention to details regarding the optimal technique needed to achieve this relative performance. Routine MRI examination of the liver should include both single shot T2-weighted and breath-hold T1-weighted images (2), as well as gadolinium enhancement with the acquisition of multiple phases. The T1-weighted precontrast images must include in-phase and out-of-phase acquisitions to assess hepatic lipid or iron content. T1-weighted pre- and postgadolinium enhanced images are acquired using a fat-suppressed three-dimensional gradient-echo (3D GRE) sequence (3). These images are most commonly acquired in the axial plane with approximately 2 mm in-plane resolution and 2–3 mm resolution in the z-axis. Using various acceleration techniques, including parallel processing and under sampling, 3D GRE images covering the entire liver from the lung bases to below the kidneys can be acquired under 15 s during a single breath hold. Dynamically enhanced postgadolinium images are acquired to characterize tumors and diffuse liver disease. The timing of the arterial phase images is critical to providing unique diagnostic information for determining the perfusion characteristics of hepatic lesions and revealing hemodynamic changes related to active liver disease. The venous and delayed recirculation phase images, sometimes referred to as “equilibrium” phase images, are used for detecting other characteristic features delineating different tumor types and for grading hepatic fibrosis related to chronic liver disease. In chronic liver disease, dynamic postgadolinium images are critical for the detection and characterization of regenerative or dysplastic nodules and hepatocellular carcinoma. The same sequences that are useful for liver evaluation allow the comprehensive evaluation of all soft tissues of the abdomen and the depiction of most of the important diseases, and thus, they facilitate the use of a universal protocol for abdominal imaging.

Various etiologies have been described for diffuse liver disease (4). This review article discusses acute and chronic liver disease processes in light of the MRI features and techniques that are used for the evaluation of diffuse liver diseases.

## Active inflammation

Active liver disease can result from several etiologies, including idiopathic, drug-induced, viral, and alcoholic hepatitis, and gallstone bile duct obstruction (5–7) that lead to active inflammation of various degrees and patterns. At this time, MRI is the only imaging technique that has been shown to be sufficiently sensitive for the detection of active

Department of Medical Imaging (D.R.M. ✉ [dmartin@radiology.arizona.edu](mailto:dmartin@radiology.arizona.edu)), University of Arizona College of Medicine, Tucson, Arizona, USA.

Received 25 April 2013; revision requested 22 May 2013; final revision received 21 November 2013; accepted 22 November 2013.

Published online 2 April 2014.  
DOI 10.5152/dir.2014.13170

liver disease (7, 8). Until now, we have relied on serum levels of liver enzymes in combination with percutaneous liver biopsy. The most sensitive MRI images are the postgadolinium breath-hold spoiled GRE images that are acquired during the arterial phase (Figs. 1, 2) (5, 7). A recent study showed that this abnormal enhancement becomes more pronounced and can persist into the venous and delayed phases as the severity of disease increases and can resolve in cases where the active inflammation subsides (7). Furthermore, the timing of the arterial phase critically determines the sensitivity to mild active liver disease (7). By performing short acquisition T1-weighted GRE imaging every 5 s after administration of gadolinium to a patient who has mild

active liver disease, the authors found that irregular liver enhancement was detectable only during the time when the portal veins were filling with contrast; the hepatic veins were unenhanced, corresponding to the first pass perfusion of the contrast agent through the hepatic parenchyma. In cases of mild hepatitis, images that are acquired before portal venous filling were too early, and images that were acquired when the hepatic veins were filled were too late.

Nonalcoholic steatohepatitis is a type of hepatitis believed to be due to multiple factors, including intracellular lipid accumulation within hepatocytes that leads to oxidative stress and inflammation. This disease has a strong association with obesity and

has a risk of progression to chronic hepatitis (Fig. 3), cirrhosis, and hepatocellular carcinoma. Nonalcoholic steatohepatitis is an important health concern in the USA and is increasingly important in other developed and developing nations. MRI offers the added value of providing a diagnostic test with greater sensitivity and specificity for the detection of fatty liver. MRI may be used as a diagnostic aid in patients who have equivocal elevation of liver enzyme levels and nonspecific symptoms and in patients who are suspected of having fatty liver disease. Nonalcoholic fatty liver disease is a disorder of abnormal lipid accumulation within the hepatocytes. In a subset of patients, active liver disease develops and can lead to fibrosis and

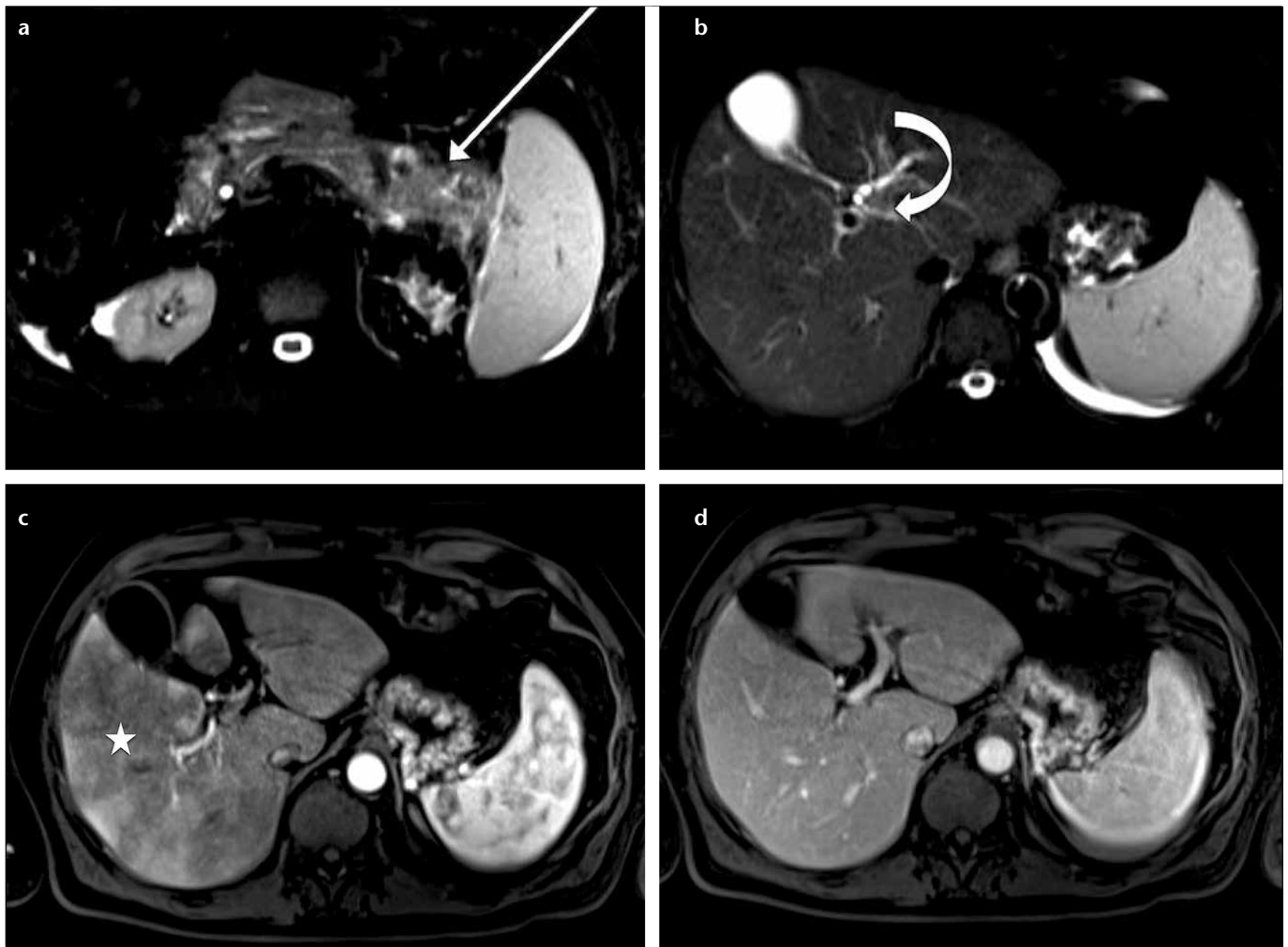


**Figure 1. a–d.** Altered liver hemodynamics due to extrahepatic etiology in a patient without active liver disease. Axial T2-weighted images (a, b) show increased T2 signal in and surrounding the pancreas (*arrow*) consistent with acute pancreatitis. There is also mild periportal edema (b, *curved arrow*). Axial T1-weighted postcontrast image shows heterogeneous enhancement (*star*) of the liver on the arterial phase (c), which normalizes on the venous phase (d). These findings are the result of hemodynamic factors released by the pancreas into the portal venous supply to the liver. We find that this effect on liver perfusion occurs with other inflammatory processes of the digestive system.

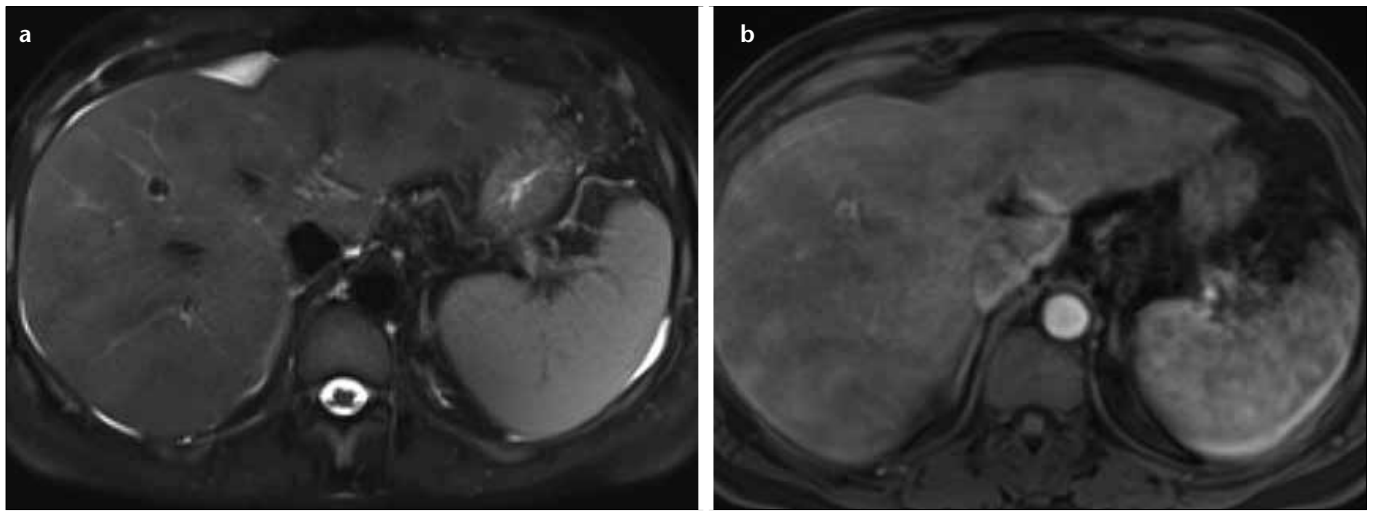


**Figure 2. a, b.** Active liver disease. Axial T2-weighted image with fat saturation (**a**) demonstrates periportal edema and perihepatic ascites. Axial T1-weighted postcontrast image (**b**) demonstrates heterogeneous enhancement of the liver on the arterial phase. These findings are suggestive for active liver disease in this patient with viral hepatitis, as previously described.

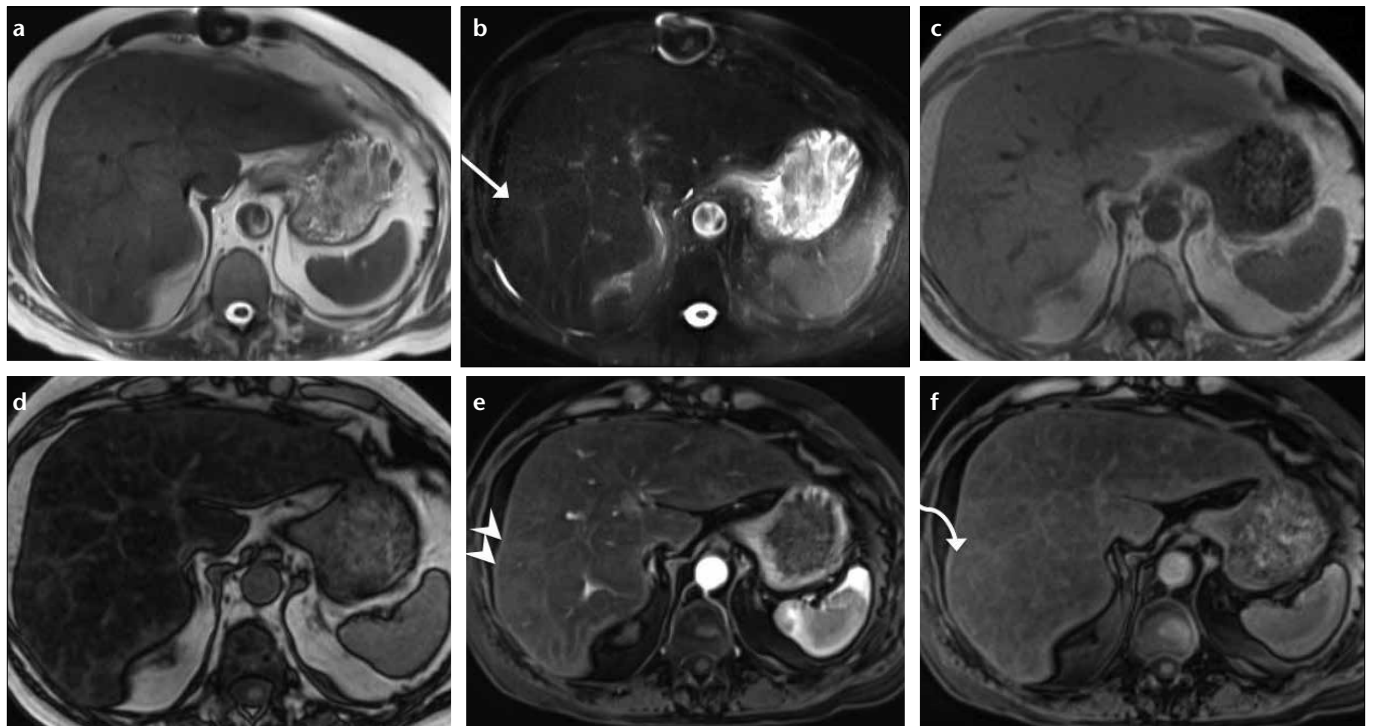


**Figure 3. a–f.** Active chronic liver disease with moderate severity. Axial T2-weighted images without (**a**) and with fat saturation (**b**) show increased T2 signal (**b**, *arrow*) in the liver with mild periportal edema, more marked in the areas of the most advanced disease involving the right lobe of liver. The central liver and left lobe have less advanced disease and are undergoing compensatory hypertrophy—growing in size to develop increased function to compensate for the diminished function in the more diseased regions. Axial in-phase (**c**) and out-of-phase (**d**) images demonstrate loss of signal on the out-of-phase image relative to in-phase image, indicating steatosis. Axial T1-weighted postcontrast images (**e**, **f**) demonstrate mild heterogeneous enhancement (*arrowheads*) of the liver on the postcontrast arterial phase (**e**), consistent with active disease. There are nonuniform linear enhancing bands extending perpendicular to the liver capsule with progressive uptake of contrast agent (**f**, *curved arrow*). Overall, these findings are diagnostic of fatty liver with disease progression and changes of moderately severe chronic liver disease.

chronic liver disease. MRI is well suited for detecting and quantifying the fat fraction in the liver tissue using multiple-echo Dixon or spectroscopy techniques (9, 10). Abnormal arterial enhancement is suggestive of active liver disease (Fig. 3), although no systematic demonstration of sensitivity or

specificity of MRI for early active liver disease and nonalcoholic steatohepatitis has yet been shown. The ability to detect changes related to fibrosis using MRI is discussed in the following section on chronic liver disease.

Multiple causes of transient hepatic perfusion abnormalities have been de-

scribed; however, in cases that present clinically with right upper quadrant pain and abnormal liver arterial phase perfusion, active liver disease should be a diagnostic consideration (7). We have found that hepatic perfusion abnormalities may arise from active liver disease or from extrinsic inflammatory

processes that have blood drainage to the liver, including pancreatitis or inflammatory disease affecting the bowel. However, the levels of liver enzymes are usually normal, and no other findings of liver disease, or active hepatitis, are found in these cases. The liver perfusion abnormalities should improve after resolution of the extrahepatic source of hemodynamic factors. It may be argued that patients who have right upper quadrant abdominal symptoms should be examined preferentially by MRI over CT. MRI has potential relative strengths with respect to contrast sensitivity and can provide excellent temporal resolution because of the small contrast volume used, in combination with a short acquisition window allowing capture of transient perfusion defects. Additionally, the safety profile of gadolinium agents and non-ionizing radiation imaging for a multiphase examination are attractive characteristics of MRI.

The causes of heterogeneous liver enhancement in active liver disease have not been fully determined. Hypothetically, it may be that the areas of relative arterial phase hyperenhancement represent regions of abnormality. In this case, periportal inflammation may lead to increased intraparenchymal pressure and compress differentially the lower pressure intrahepatic branches of the portal vein leading to preferential segmental hepatic arterial perfusion. Alternatively, the inflammation may lead to altered vascular regulatory effects, with vasodilation and increased hepatic arterial flow to the involved regions. Pathologic correlation is challenging given that histopathologic correlation lacks the ability to determine active pathophysiologic *in vivo* processes that are involved in hemodynamics, an advantage that is inherent to contrast enhanced imaging.

#### **Technical considerations: tips and tricks**

In the latest generation MRI systems, timing of the arterial phase acquisition in relation to contrast administration can be automated with the objective of improving uniformity of results across patients and across different imaging centers. One optimized approach has

relied on using a real-time imaging acquisition to watch the injected contrast bolus arriving at a trigger point; the trigger point is the time when the breath hold T1-weighted 3D GRE sequence is initiated. The arrival of contrast at the level of the aortic origin of the celiac artery has proven to be a practical trigger point and has been used to formulate strategies such as the “automated breath-hold liver examination” technique that has been described previously (11). The parameters for breath-hold spoiled GRE arterial phase acquisition that must be taken into account include design of the 3D GRE sequence. For example, a sequence using a simple linear ordering of k-space, which fills central k-space in the middle of the acquisition time, will acquire most of the information used to construct the contrast information within the image during approximately the middle 20%–30% of the total acquisition time. For example, a linear acquisition with a total acquisition time of 20 s will acquire most of the contrast information between 7–13 s into the acquisition. The next consideration should be the time at which peak concentration of the first pass of contrast agent perfuses the liver from the arterial supply. The timing of the arterial phase 3D GRE should correspond to the time of peak concentration. If, for example, the acquisition scan time is decreased by 5–15 s, then the delay time between the start of the injection and the start of the acquisition should be increased by 2–3 s to realign the peak of contrast concentration with a central k-space acquisition time window of 5–10 s after the start of the acquisition. Note also that the total time of the contrast window narrows. If the start of timing is taken from the start of the contrast infusion into an arm vein, the time variability between patients becomes very large relative to the narrow time window available for central k-space acquisition. Arm vein variability is in the range of tens of seconds between patients (11), while the acquisition time window is in the range of seconds. An earlier technique to overcome this challenge has been to use a test bolus infusion, but this entails additional steps, a preinjection of contrast, and the potential errors from

the added complexity of calculations. A real time bolus trigger technique improves efficiency of the overall MRI exam, provided the trigger methodology is reliable. Using the detection of contrast bolus at the origin of the celiac artery as the trigger point provides a method that reduces the variability to a range of seconds; the time difference between arrival at the celiac artery and liver arterial peak perfusion averages 8 s with small variability between patients (11). This method will ensure that the centerlines of k-space are filled at the peak of the hepatic arterial tissue perfusion phase. Another consideration is the k-space algorithm used by the 3D GRE acquisition. If in lieu of a linear model, an elliptocentric model is used, for example, the central k-space may be acquired at the beginning, at the end or even in the middle of the overall acquisition. Radial 3D GRE methods may sample k-space throughout the entire acquisition. While this may appear complex, newer systems can provide automated on-the-fly optimized acquisition times based on bolus trigger technique, minimizing errors that may arise from operator sources. Furthermore, the most recent generation of MRI scanners allow for 3D GRE acquisitions in less than 15 s. With such a short acquisition time, the requirement to account for differences in k-space algorithms becomes less significant because the overall acquisition time becomes shorter than the time of the bolus transit time.

#### **Chronic liver disease and cirrhosis**

A major complication of chronic liver disease is cirrhosis and hepatocellular carcinoma (12). In Western nations, the most common etiology has been alcohol-induced hepatitis; however, viral hepatitis has become the most common cause over the past 20 years. Globally, viral hepatitis remains the most common cause of chronic liver disease, hepatic fibrosis leading to cirrhosis, and hepatocellular carcinoma.

MRI signal characteristics of fibrosis is progressive enhancement on delayed images within the fibrotic bands of tissue that surrounds regenerative nodular liver that does not show delayed contrast uptake (13); this pattern of contrast enhancement results from

leakage of the gadolinium contrast agent from the intravascular into the interstitial space within the fibrotic regions, but without accumulation in the regenerative nodules. (14). This is a favorable characteristic of extracellular gadolinium-based chelate agents, which behave much like a histological stain for fibrotic tissues. On subsequent delayed interstitial phase images, acquired at range of 3–5 min after gadolinium administration, strong quantitative correlation between delayed phase liver enhancement pattern and hepatic fibrosis has been reported. The typical patterns of hepatic fibrosis include fine reticular and coarse linear patterns, with the fibrotic bands outlining foci of regenerative nodules. The earliest region of liver that develops detectable fibrosis is usually the subcap-

sular region of the anterior segments V and VIII of the right lobe (Fig. 4). The fibrotic bands of tissue frequently also show elevated T2-weighted signal (Figs. 5, 6), possibly due to altered hemodynamics or lymphatic dynamics and fluid retention. We have previously used computational fluid dynamics to show that the right hepatic lobe preferentially receives blood return from the superior mesenteric vein, while the left lobe is predominantly supplied by the splenic return. This may account for more advanced disease occurring where greater metabolic and oxidative stress may be present, in the right lobe tissue receiving nutrients from the small bowel. Different innovative MRI techniques are under active development for quantifying hepatic fibrosis, as a surrogate for histological markers

of hepatic fibrosis. Extracellular uptake of gadolinium-based contrast agents (GBCA) in hepatic fibrosis has been shown to correlate with the histological stage of fibrosis (14). A technique to further increase contrast for evaluation of hepatic fibrosis has used a combination of contrast agents, such as concurrent administration of an extracellular GBCA and ultra small superparamagnetic iron oxide (USPIO). This approach is based on the concept that functional or regenerative liver retains reticuloendothelial cells that will take up the iron contrast agent while fibrotic tissue will not. GBCA accumulates within the intervening fibrotic tissue. The combined effects of the iron enhancing signal in regenerative liver and the GBCA increasing signal in fibrotic tissue lead to increased contrast

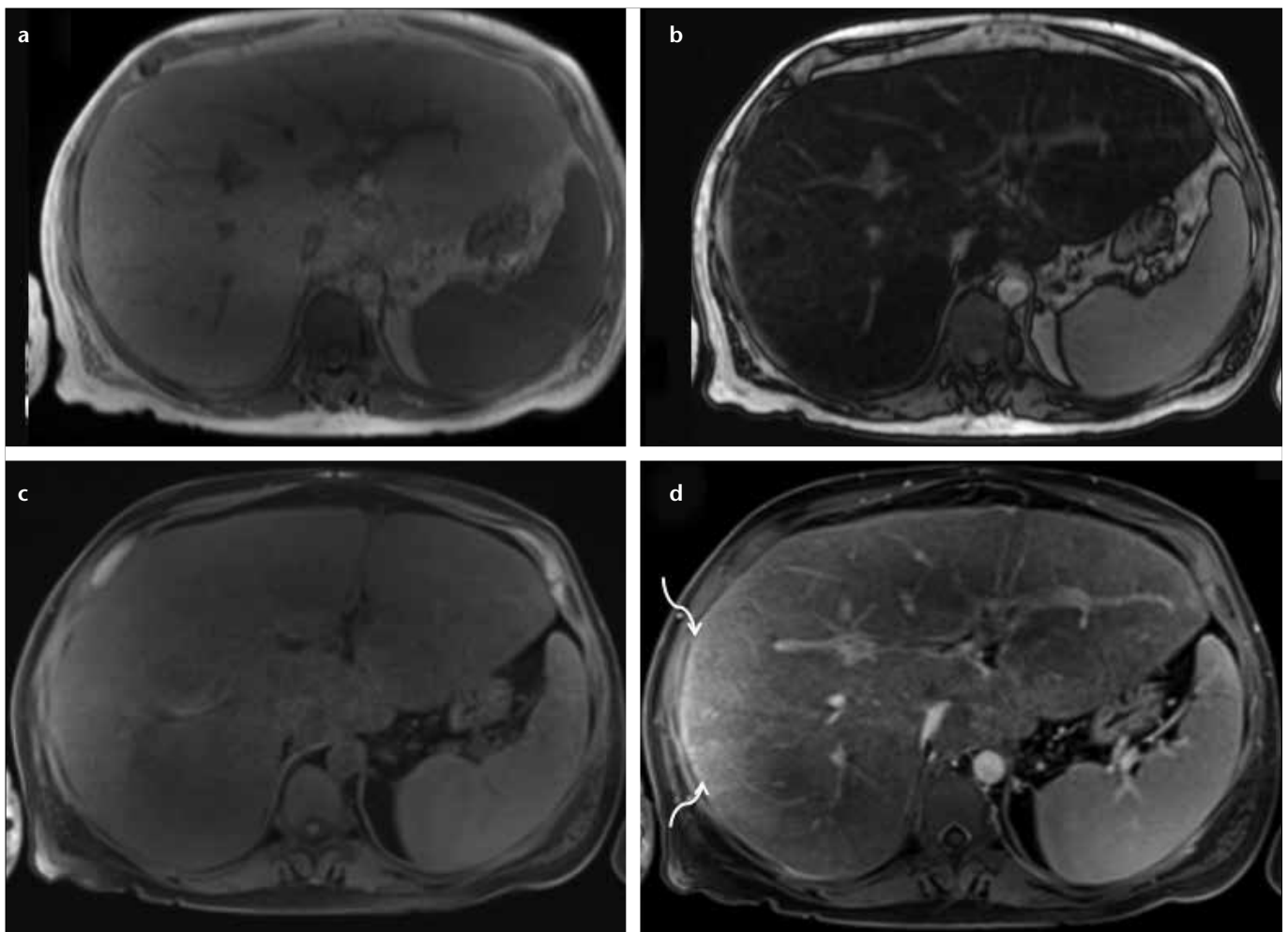


**Figure 4. a–d.** Chronic liver disease with moderate severity. Axial in-phase (a) and out-of-phase (b) images show loss of signal intensity of the liver on the out-of-phase image relative to the in-phase image, consistent with hepatic steatosis. Axial T1-weighted precontrast image (c) demonstrates rounded liver contours. Axial delayed postcontrast image (d) demonstrates nonuniform linear enhancing bands extending perpendicular to the liver capsule (*curved arrows*) and has been found to be a marker in chronic liver disease.

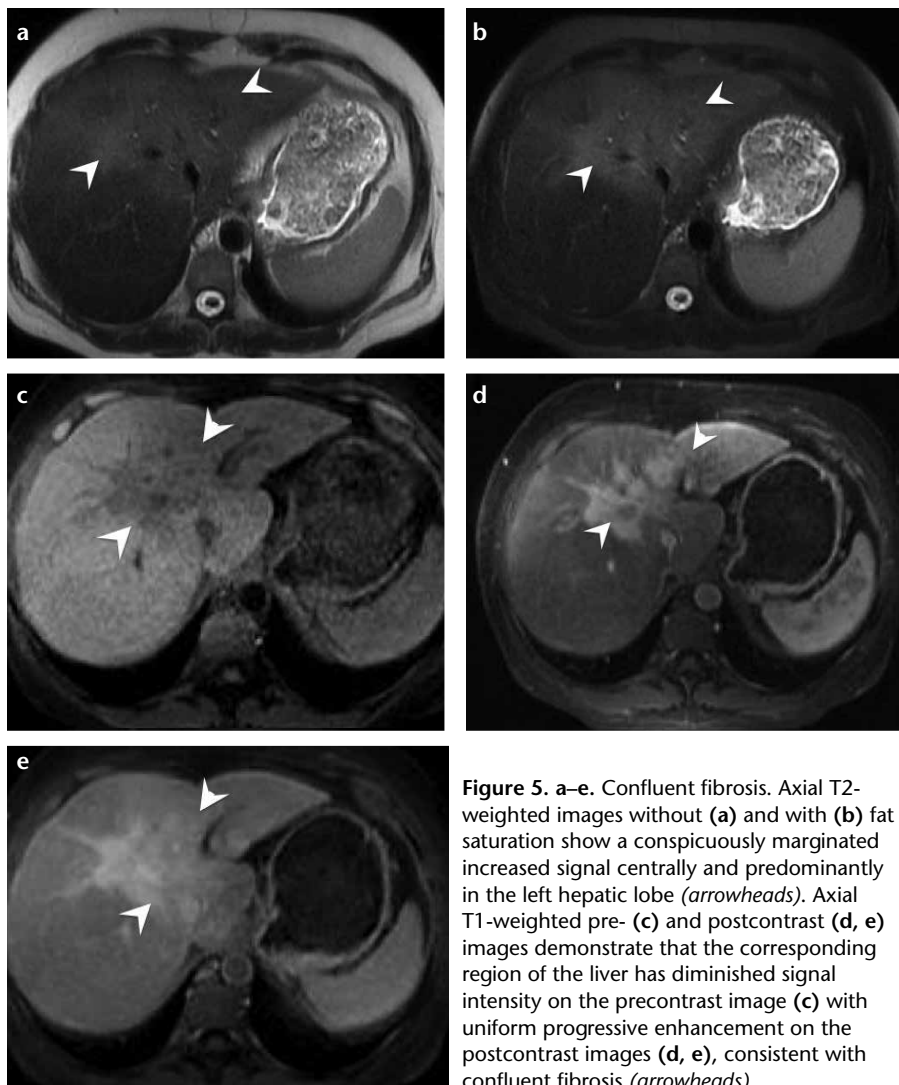


**Figure 5. a–e.** Confluent fibrosis. Axial T2-weighted images without (a) and with (b) fat saturation show a conspicuously marginated increased signal centrally and predominantly in the left hepatic lobe (arrowheads). Axial T1-weighted pre- (c) and postcontrast (d, e) images demonstrate that the corresponding region of the liver has diminished signal intensity on the precontrast image (c) with uniform progressive enhancement on the postcontrast images (d, e), consistent with confluent fibrosis (arrowheads).

differentiation between liver and fibrotic tissue. However, USPIO agents are no longer readily available for clinical use at this time. As an alternative, the use of the hepatocyte uptake agent gadoxetate disodium will result in contrast accumulation within regenerative liver nodules (15). Because liver cell function may vary with different stages of disease, there is potential for variable contrast between liver regenerative nodules and surrounding fibrosis, causing the nodules to appear either hyper- or isointense relative to the fibrosis (15).

Diffusion-weighted imaging (DWI) has been proposed for assessing hepatic fibrosis. DWI is a method for determining relative levels of restriction to the movement of water within the imaged tissues. In hepatic fibrosis, free unbound water should be diminished,

and the accumulation of fibrosis should cause a reduction in the amount of water proton diffusion in affected liver tissue. However, DWI is not showing reliable and quantitative sensitivity for different stages of fibrosis.

MR elastography is based upon the application of an external displacement pressure over the liver timed to trigger phase-sensitive MRI. The group of Richard Ehman from the Mayo Clinic (16) has developed this technique, and the MR elastography system is now commercially available and configured to function on most MRI systems. It requires placement of a compression paddle along the right upper quadrant of the abdomen, overlying the lower right hemithorax. Tubing extends from a speaker placed within a closed system outside of the MRI room and connected to the compression paddle with tub-

ing that is passed through a wave-guide to avoid external radiofrequency leakage. The driver for the enclosed speaker is connected to an external trigger in the MRI equipment room to achieve controlled, coordinated triggering of pressure pulses generated from the speaker with the MRI excitation-image acquisitions. These acquisitions are based on GRE-producing phase contrast changes from tissue movement that can be measured and translated into color-encoded wave dispersion maps (Fig. 7). The spleen can be seen to have lesser elasticity in the patient with chronic liver disease, which may be a result of portal hypertension (17). By acquiring images with increasing time delays over several pressure pulses, the displacement compression waves traversing the liver may be determined, and the tissue stiffness measured (16). MR elastography has been shown to derive stiffness measures that correlate with the different stages of fibrosis on histology. It should be noted that an analogous technique using ultrasound combined with mechanical operator applied pressure over the liver, to create the displacement, has also been found to correlate with tissue stiffness and hepatic fibrosis (Fig 7). Further validation and relative comparison of these techniques remains an area of active study.

MR spectroscopy is most commonly used to assess signals from hydrogen ( $^1\text{H}$ ) and phosphorus ( $^{31}\text{P}$ ). An increased hepatic phosphomonoester signal measured by MR spectroscopy and an increasing phosphomonoester/phosphodiester ratio have been reported (18); however, the relationship between phosphodiester and fibrosis is not well understood.

A more recent MR spectroscopy technique (19) has been proposed using the combination of a highly spatially sampled linear MR spectroscopy acquisition followed by post-processing with mapping of the magnitude of the signal against the wavelength. This yielded an analysis that corresponds to tissue features and appears to correlate with the degree of hepatic fibrosis in human livers (Fig. 7).

Portal hypertension may result from obstruction at presinusoidal, sinusoidal, or postsinusoidal sites, or a com-

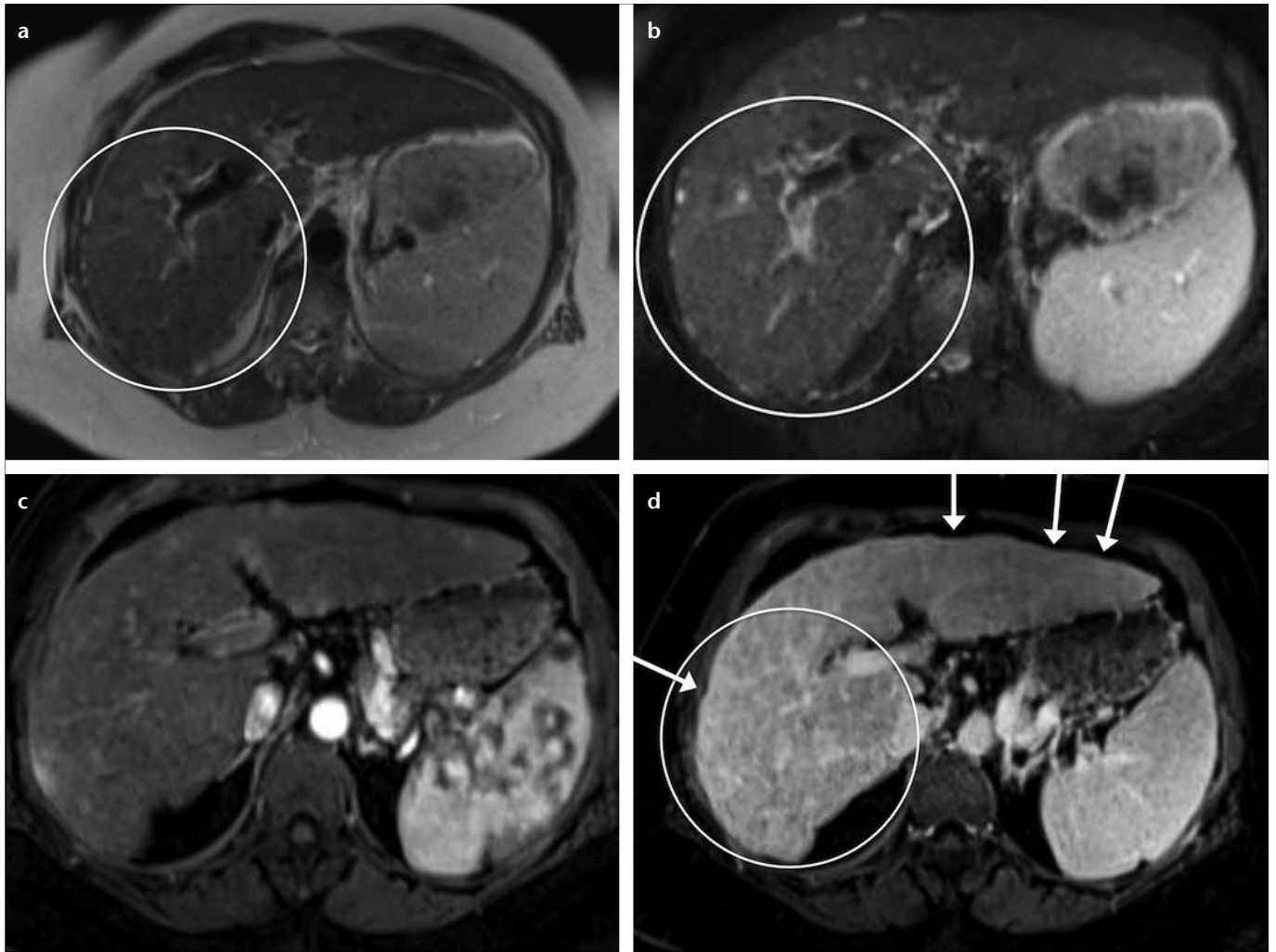


**Figure 6. a–d.** Chronic liver disease with highest severity. Axial T2-weighted images without (a) and with (b) fat saturation show elevated signal in the liver, most evident in the regions most affected by chronic liver disease, which coincides with the right lobe of liver (circles). Axial T1-weighted postcontrast images (c, d) demonstrate a coarse reticular pattern of enhancement with thickened linear enhancement that extends to the capsule along the periphery of the liver and that becomes most conspicuous on the postcontrast delayed phase images (d), consistent with severe fibrosis. Note that the elevated T2 signal corresponds to the late-enhancing fibrotic reticular pattern tissue that surrounds small regenerative nodular liver. Unlike fibrotic tissue elsewhere in the body, fibrotic liver elements tend to have an elevated T2 signal; a histopathological correlate has not yet been shown for this feature of hepatic fibrosis. Note also the areas of coarse linear enhancing peripheral fibrosis on delayed phase postcontrast 3D GRE that extend to the liver capsule and correspond to foci of liver surface retraction (arrows). This leads to the nodular surface contour visualized on cross-sectional imaging.

bination thereof, and corresponds to portal or hepatic vein abnormalities, hepatic fibrosis, or mixed diseases. With MR images optimized for visualizing changes related to portal hypertension that are obtained on equilibrium phase 3D GRE images with fat suppression in early or mild portal hypertension, MRI shows dilation of the portal vein and possibly the splenic vein. In more severe and chronic cases, the portal vein may become occluded and narrow or inconspicuous. In patients with portal vein thrombosis, cavernous transformation may occur, as evidenced by replacement

of a portal vein by numerous typically smaller caliber collateral veins within the porta hepatis. Porto-systemic collaterals can form, bypassing the liver, and are seen as retroperitoneal vessels in increased number and size in the region of the splenic hilum, gastro-hepatic ligament, paraesophageal region, and with demonstration of spleno-renal venous connections. Canalization of the paraumbilical vein can be detected as a vessel, sometimes massive, that extends from the left portal vein anteriorly along the falciform ligament toward the anterior abdominal wall umbilical region. Ascites typically

develops in association with more advanced portal hypertension and hypoproteinemia, due to liver dysfunction, appearing as simple uniform high-signal T2-weighted fluid in the free intraperitoneal space.

Regenerative nodules occur in the setting of chronic liver disease (10) and represent relatively more normal hepatic parenchyma that derives its major blood supply from the portal venous system. Thus, these nodules maximally enhance during the portal venous phase and are usually less than 1 cm in diameter. These nodules can accumulate iron and appear

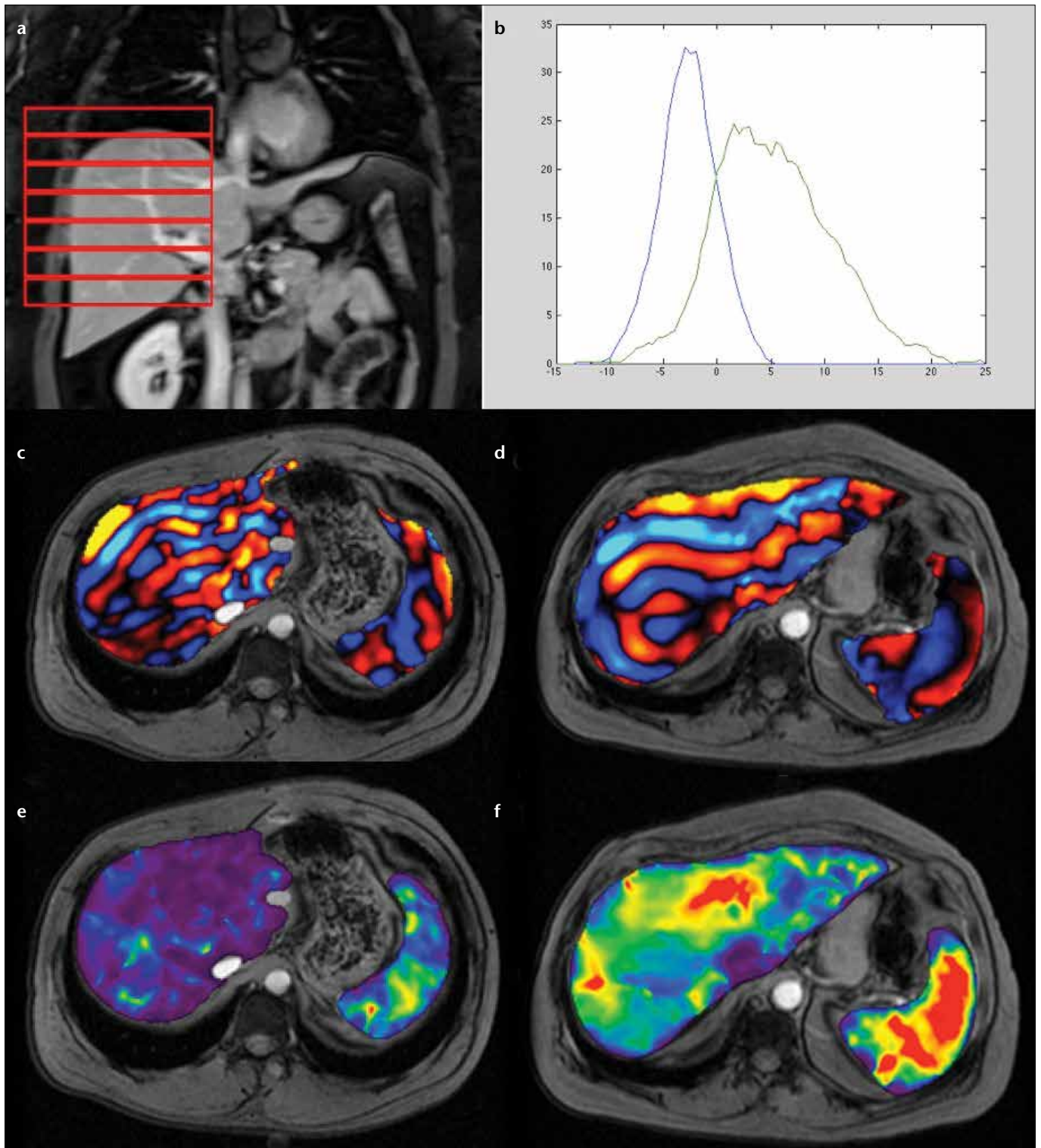


**Figure 7. a–f.** Newer methods for quantifying liver features related to chronic liver disease and fibrosis. Coronal T1-weighted postcontrast image (a) allows a fine feature analysis using interleaved one-dimensional spectroscopy prisms representing selectively excited internal volumes that are aligned with the coronal plane and localized to the right lobe of the liver. Histogram plot (b) of discriminant values derived from the MR spectroscopy wavelength data output of normal (blue) and fibrotic livers (green). These data were extracted from highly spatially sampled MR spectroscopy and the spectrum of the wavelengths and magnitudes were plotted to mathematically analyze differences between normal and abnormal liver. Note that the green curve, acquired from fibrotic liver, is significantly different from normal. Although new, MR spectroscopy feature analysis is a promising technique for assessing changes in tissue architecture down to submillimeter resolution. Axial MR elastography images of normal (c) and fibrotic (d) liver showing shear wave imaging with the corresponding normal (e) and fibrotic (f) liver calculated elastogram images. The shear stiffness values are color-encoded, with purple-blue representing the lowest range of stiffness and green-red representing the highest. Note that the normal liver has shear waves propagating closer together (c vs. d). The corresponding calculated stiffness showed an average value of 1.8 kPa (e) vs. over 5 kPa (f) in a patient with chronic liver disease and advanced stage fibrosis.

to have a low signal on both 3D GRE T1-weighted and single shot fast spin echo T2-weighted images, with little enhancement appreciated on GB-CA-enhanced 3D GRE images. Dysplastic nodules are premalignant and are believed to have the potential to transform into progressively higher grades of dysplasia and, finally, into hepatocellular carcinoma. Dysplastic nodules typically are larger than regenerative nodules and can be seen to grow over a period of weeks or months. These lesions can overlap with hepatocellular carcinoma and may show mildly elevated T1-weighted and low T2-weighted signals. Features that help to differentiate hepatocellular carcinoma include transient, marked arterial phase postgadolinium enhancement, capsular peripheral rim enhancement on venous and equilibrium phase images, and dimension greater than 2 to 3 cm. A fraction of hepatocellular carcinoma shows elevated T2-weighted signal on single shot technique, but this is not seen in the regeneration of dysplastic nodules and is therefore considered a marker of malignancy. It may be that higher-grade dysplastic nodules overlap more with the hepatocellular carcinoma features; however, this distinction may be of small clinical significance because higher-grade dysplastic nodules have the potential to transform into hepatocellular carcinoma rapidly.

### Conclusion

Current and developing MRI techniques for detecting and quantifying biomarkers of diffuse liver disease are poised to provide game changing technology for diagnosis, monitoring of disease, and for therapy development.

### Conflict of interest disclosure

The authors declared no conflicts of interest.

### References

1. Semelka RC, Martin DR, Balci C, et al. Focal liver lesions: comparison of dual-phase CT and multisequence multiplanar MR imaging including dynamic gadolinium enhancement. *J Magn Reson Imaging* 2001; 13:397–401. [\[CrossRef\]](#)
2. Naganawa S, Jenner G, Cooper TG, et al. Rapid MR imaging of the liver: comparison of twelve techniques for single breath-hold whole volume acquisition. *Radiat Med* 1994; 12:255–261.
3. Rofsky NM, Lee VS, Laub G, et al. Abdominal MR imaging with a volumetric interpolated breath-hold examination. *Radiology* 1999; 212:876–884. [\[CrossRef\]](#)
4. Chundru S, Kalb B, Arif-Tiwari H, Sharma P, Costello J, Martin DR. MRI of diffuse liver disease: the common and uncommon etiologies. *Diagn Interv Radiol* 2013; 19:479–487.
5. Matsui O, Kadoya M, Takashima T, et al. Intrahepatic periportal abnormal intensity on MR images: an indication of various hepatobiliary diseases. *Radiology* 1989; 171:335–348.
6. Marzola P, Maggioni F, Vicinanza E, et al. Evaluation of the hepatocyte-specific contrast agent gadobenate dimeglumine for MR imaging of acute hepatitis in a rat model. *J Magn Reson Imaging* 1997; 7:147–152. [\[CrossRef\]](#)
7. Martin DR, Seibert D, Yang M, et al. Reversible heterogeneous arterial phase liver perfusion associated with transient acute hepatitis: findings on gadolinium-enhanced MRI. *J Magn Reson Imaging* 2004; 20:838–842. [\[CrossRef\]](#)
8. Sharma P, Kitajima HD, Kalb B, et al. Gadolinium-enhanced imaging of liver tumors and manifestations of hepatitis: pharmacodynamic and technical considerations. *Top Magn Reson Imaging* 2009; 20:71–78. [\[CrossRef\]](#)
9. Reeder SB, Cruite I, Hamilton G, Sirlin CB. Quantitative assessment of liver fat with magnetic resonance imaging and spectroscopy. *J Magn Reson Imaging* 2011; 34:729–749. [\[CrossRef\]](#)
10. Pineda N, Sharma P, Xu Q, Hu X, Vos M, Martin DR. Measurement of hepatic lipid: high-speed T2-corrected multiecho acquisition at 1H MR spectroscopy—a rapid and accurate technique. *Radiology* 2009; 252:568–576. [\[CrossRef\]](#)
11. Sharma P, Kalb B, Martin DR, et al. Optimization of single injection liver arterial phase gadolinium enhanced MRI using bolus track real-time imaging. *J Magn Reson Imaging* 2011; 33:110–118. [\[CrossRef\]](#)
12. Kreft B, Dombrowski F, Block W, et al. Evaluation of different models of experimentally induced liver-cirrhosis for MRI research with correlation to histopathologic findings. *Invest Radiol* 1999; 34:360–366. [\[CrossRef\]](#)
13. Semelka RC, Chung JJ, Hussain SM, et al. Chronic hepatitis: correlation of early patchy and late linear enhancement patterns on gadolinium-enhanced MR images with histopathology initial experience. *J Magn Reson Imaging* 2001; 13:385–391. [\[CrossRef\]](#)
14. Martin DR, Lauenstein T, Kalb B, et al. Liver MRI and histological correlates in chronic liver disease on multiphase gadolinium-enhanced 3D gradient echo imaging. *J Magn Reson Imaging* 2012; 36:422–429. [\[CrossRef\]](#)
15. Cruite I, Schroeder M, Merkle EM, Sirlin CB. Gadoxetate disodium-enhanced MRI of the liver: part 2, protocol optimization and lesion appearance in the cirrhotic liver. *AJR Am J Roentgenol* 2010; 195:29–41. [\[CrossRef\]](#)
16. Venkatesh SK, Yin M, Ehman RL. Magnetic resonance elastography of liver: technique, analysis, and clinical applications. *J Magn Reson Imaging* 2013; 37:544–555. [\[CrossRef\]](#)
17. Nedredal GI, Ehman R, Nyberg SL. Portal hypertension correlates with splenic stiffness as measured with MR elastography. *J Magn Reson Imaging* 2011; 34:79–87. [\[CrossRef\]](#)
18. Talwalkar JA, Kamath PS, Ehman RL, et al. Magnetic resonance imaging of hepatic fibrosis: emerging clinical applications. *Hepatology* 2008; 47:332–342. [\[CrossRef\]](#)
19. Chundru S, Martin D, Jezzard P. Novel MR fine texture spectroscopy technique enabling visualization of fine structures: fibrosis detection in chronic liver disease. Paper presented at: ISMRM; May 8, 2012; Melbourne, Australia.